Journal of The Electrochemical Society, **153** (6) A1246-A1253 (2006)
0013-4651/2006/153(6)/A1246/8/$20.00 © The Electrochemical Society

Interfacial Properties of the a-Si/Cu:Active–Inactive Thin-Film Anode System for Lithium-Ion Batteries

J. P. Maranchi,[a] A. F. Hepp,[b] A. G. Evans,[c] N. T. Nuhfer,[a] and P. N. Kumta[a,*,z]

[a]*Department of Materials Science and Engineering, Carnegie Mellon University, Pittsburgh, Pennsylvania 15213, USA*
[b]*NASA Glenn Research Center, Photovoltaic and Space Environments Branch, Cleveland, Ohio 44135, USA*
[c]*Department of Materials, University of California, Santa Barbara, California 93106, USA*

Amorphous silicon thin films deposited on copper foil have been observed to exhibit near theoretical capacity for a limited number of cycles. The films, however, eventually delaminate, leading to failure of the anode. In order to better understand the mechanism of capacity retention and the ultimate failure mode of a model brittle active:elastic/plastic inactive anode system, the films were subjected to in situ adhesion tests while observing the film surface using scanning electron microscopy. Atomic force and transmission electron microscopy, and electrochemical cycling were conducted to analyze the emerging morphology of the films during cycling. The adhesion of the as-deposited Si film to the Cu substrate was measured to ~7.7 J/m^2, reflecting a weak interface adhesion strength. Plastic deformation of the underlying Cu substrate combined with a ratcheting mechanism is proposed to occur in the Si:Cu system, with delamination failure mode occurring only after the formation of an interface imperfection. From the analysis of slow rate cycling experiments, nucleation of a lithium compound based on the interdiffusion of Si and Cu is identified as the most probable cause of the ultimate delamination failure of the deposited film.
 [DOI: 10.1149/1.2184753]

Manuscript submitted July 15, 2005; revised manuscript received December 19, 2005. Available electronically May 2, 2006.

Much research interest is ongoing toward developing lightweight high-capacity anode materials for lithium-ion batteries to replace the conventional carbon-based anodes currently used in commercial batteries. Volumetric expansion and contraction during lithiation has been identified as the major issue preventing the utilization of new anode materials such as elemental tin or Si, which showed promise due to their potential for high capacity.[1] In an effort to reduce the negative effects associated with the expansion/contraction, multicomponent tin-containing oxides were studied which yielded significant improvements in cyclability.[2] Unfortunately, the tin oxide-based anode systems suffered from very large 1st cycle irreversible capacity.[3] Nonoxide-based inactive materials have been used with the hope that they could withstand the volumetric stresses of the active phases.[4] Promising results using metallic alloys containing active and inactive phases have been reported.[1,3-6] Other researchers recognized the importance of small grain size along with a ductile inactive phase in order to stabilize the capacity of alloy-type anodes.[7] Although many groups have focused on a variety of active/inactive material combinations, none of the systems studied have managed to achieve commercial status. There is, therefore, a need for continued research to achieve the much-desired breakthrough for identifying alternate anode materials. This requires the undertaking of a fundamental study of the active–inactive interfaces, the failure mode, and interface dynamics in order to identify a viable potential solution to the problem of volume-expansion-induced stresses, leading to the failure of the anode electrode. The execution of such a fundamental study using traditional anode fabrication methods becomes extremely daunting due to the presence of binders and additives, further adding to the complexity of the interface. As a result, it becomes extremely difficult to predict the interface characteristics leading to failure of the electrode.

A thin film of active material on an inactive metallic substrate provides an excellent anode vehicle for studying the volumetric and potentially irreversible changes occurring in the system as a result of electrochemical cycling. In situ atomic force microscopy (AFM) has been used extensively to study the cycling behavior of Sn, Si, Al, and alloy films deposited on highly polished stainless steel substrates or Cu-coated stainless steel substrates.[8,9] Researchers have also used scanning electron microscopy (SEM) to identify annealing as a process parameter that could be used to improve the properties of Fe–Si multilayer thin films deposited on Cu substrates coated with a Ti adhesion promotion layer.[10] Although these studies demonstrated the potential of the alloy-type anode systems and validated the need for further study to be conducted on such systems, there has been no focused study targeted on the characterization of the active/inactive interface. Barring complete crumbling of the active material, the active/inactive interface is the most important feature in any alloy-type anode system and warrants detailed examination.

In this paper, the interfacial properties of a model active/inactive system comprised of an amorphous silicon thin film deposited on a polycrystalline Cu foil substrate are examined for the first time. This research was motivated by our previous study wherein high capacity and retention up to 30 cycles was observed in a 250-nm a-Si thin film sputter-deposited on a Cu foil.[11] Various analytical techniques such as in situ SEM tensile testing and cross-sectional SEM and transmission electron microscopy (TEM) have been employed to gain fundamental information about the as-deposited adhesion strength in the a-Si/Cu system, as well as morphological changes occurring in the system during electrochemical cycling. The results of the analyses suggest plastic deformation of the underlying substrate combined with a ratcheting mechanism[12-14] that appears to occur upon repeated volumetric cycling of the active material, ultimately causing failure of the deposited film. Based on this study, methods to improve the behavior at the active/inactive interface of a lithium-ion battery anode system have been proposed.

Experimental

Nanoscale and mesoscale films of Si were prepared as described previously[11] by radio frequency magnetron sputtering (Perkin Elmer – 8L) from a commercial 5-in.-diam Si target (99.999%) at 200 W onto high-purity, oxygen-free 0.001-in-thick Cu foil substrates (Insulectro). The base pressure was 5×10^{-7} Torr and the working pressure was 5 mTorr argon. Presputtering was done for 30 min at 400 W prior to each deposition to remove any surface oxides from the target. Deposition of 250-nm and 1.0-μm films occurred at a rate of ~86 Å/min.

The phases present in the as-deposited films were analyzed by X-ray diffraction incorporating a state-of-the-art detector (XRD, Philips PW3040PRO, θ/θ powder diffractometer, with X'celerator detector and a Cu Kα radiation source). The microstructure and chemical composition of the films was examined using a scanning electron microscope (Philips XL30 equipped with energy-dispersive

* Electrochemical Society Active Member.
z E-mail: kumta@cmu.edu

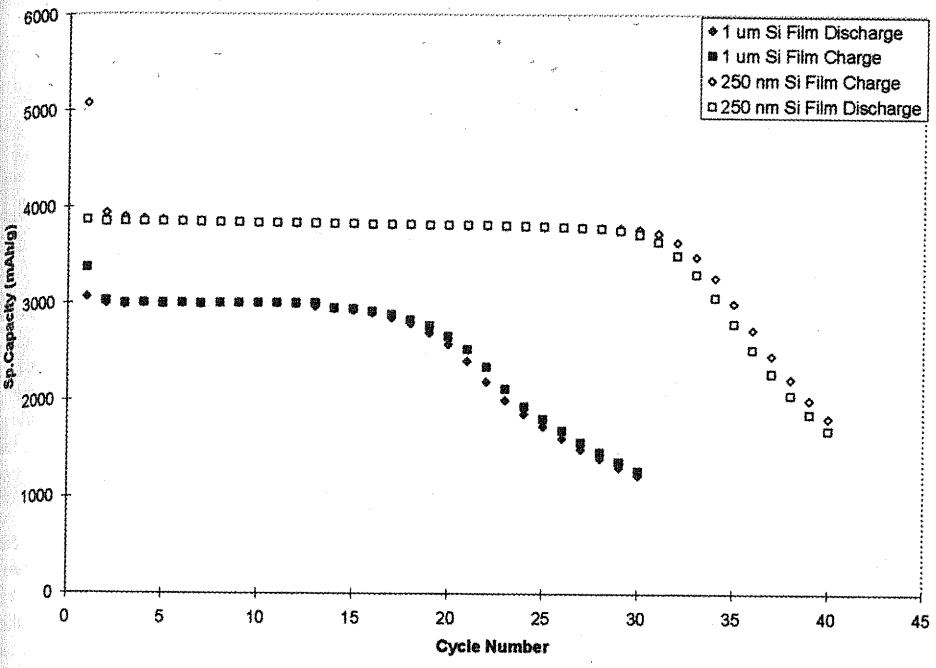

Figure 1. Comparison of galvanostatic cycling of 250-nm and 1.0-μm Si films on Cu foil (both at ~C/2.5 rate).

X-ray analysis, EDAX). The film–substrate interface was examined in detail using a high-resolution transmission electron microscope (Philips Tecnai F20 FEGTEM, 200 kV).

The electrochemical properties of the sputtered Si electrodes on Cu foil were tested using 2016 coin cells (Hohsen) and three-electrode hockey-puck-type cells. The 1-cm^2 disks were punched from the Cu foil/Si film samples, dried for >12 h in a vacuum oven (80°C), and placed inside an argon-filled glove box (Vacuum Atmospheres, Hawthorn, CA, <10 ppm O_2 and H_2O) so that construction of the batteries for testing could be performed in an inert, dry atmosphere. The half-cells were fabricated in the glove box using a punched disk of lithium foil and a microporous polyethylene separator (Tonen) or glass fiber separator (Whatman GF/D) together with the deposited films and 1 M $LiPF_6$ in ethylene carbonate/dimethyl carbonate (2:1) electrolyte (Merck). The crimped coin cells or sealed hockey puck cells were removed from the glove box, connected to a voltmeter to monitor the open-circuit voltage prior to cycling, and allowed to equilibrate a minimum of 12 h prior to constant current charge/discharge cycling (Arbin Instruments). All of the charge/discharge experiments were voltage limited between 20 mV and 1.2 V and employed constant current densities ranging from 100 to 400 μA cm^{-2} with a 60-s rest period between each charge/discharge cycle.

The interfacial fracture energy of the as-deposited a-Si film on Cu foil substrate was determined using an in situ SEM tensile testing method described in detail by Ignat.[15] The a-Si/Cu samples were cut into rectangular strips 4 × 30 mm. Two copper tabs of dimensions 20 × 10 × 0.23 mm were also prepared with 3/8-in.-diam holes to accommodate the 4-mm pins of the commercial tensile module (Kammrath & Weiss, Germany). A 4 × 5 mm section at the end of each a-Si/Cu strip was affixed using 5-min epoxy (Devcon) to the Cu tabs and allowed to cure for 1 day prior to conducting the tensile tests. Conductive paths were made between the sample and Cu tabs using Cu tape (3M). After mounting the tensile module stage in the Philips XL 30 FEGSEM, the sample was placed on the tensile stage using the 4-mm pins. A suitable area for observation near the center of the sample was selected and the experiment was initiated. All tensile experiments were computer-software-controlled and performed at a strain rate of 3 μm s^{-1}. The same area was observed during the entire experiment, and the tensile stage motor was paused at various intervals when it was considered desirable to acquire an image for obtaining structural information related to crack formation and delamination.

Results and Discussion

Electrochemical cycling.— The galvanostatic cycling results shown in Fig. 1 for a 250-nm Si thin film and 1-μm film illustrate the enormous potential of Si in terms of specific capacity compared to the conventional anode material, graphite (372 mAh/g). For example, the reversible capacity of the 250-nm film is ~3800 mAh/g for 29 cycles with a fade of 0.09% per cycle when cycled at a current density of ~C/2.5, while the reversible capacity of the 1-μm film is 3000 mAh/g for 13 cycles with a fade of 0.2% when cycled at a current density of ~C/2.5. The irreversible capacities correspond to low values of 24 and 9% for the 250-nm and 1-μm films, respectively. Unfortunately, the excellent capacity of the Cu/Si system was retained for only 29 and 13 cycles for the 250-nm and 1-μm films, respectively. In both cases, onset of the capacity fade commences in the charge half-cycle and continues to steadily fade at ~5% per cycle. In order to effectively design future thin-film anodes and propose recommendations for other bulk active-inactive anode electrodes, it is necessary to understand the ability of Si to cycle effectively, albeit for a limited number of cycles, and also determine the most likely reasons for the eventual failure of the anode system. This will help in eventually engineering the interface so that the anodes can exhibit reversible, high capacities. In order to provide an answer to these important questions, attempts were made to first examine the plan-view morphology of the postcycled Si films.

Film morphology.— The failure mode of the film is observed to occur by debonding of the Si islands from the Cu substrate, as seen in Fig. 2a for the case of the 1-μm film cycled at ~C/2.5 rate for 30 cycles. The SEM image suggests plastic deformation of the Cu substrate. For comparison, one can see similarities between Fig. 2a and the image in Fig. 2b, which shows a 250-nm Si film on Cu foil that has undergone severe tensile strain in the direction normal to the parallel cracks. One can distinguish three regions in Fig. 2a. As reported previously[11] for the 250-nm Si films cycled at a C/2.5 rate for 30 cycles, region 1 shows an area where the 1-μm Si has formed

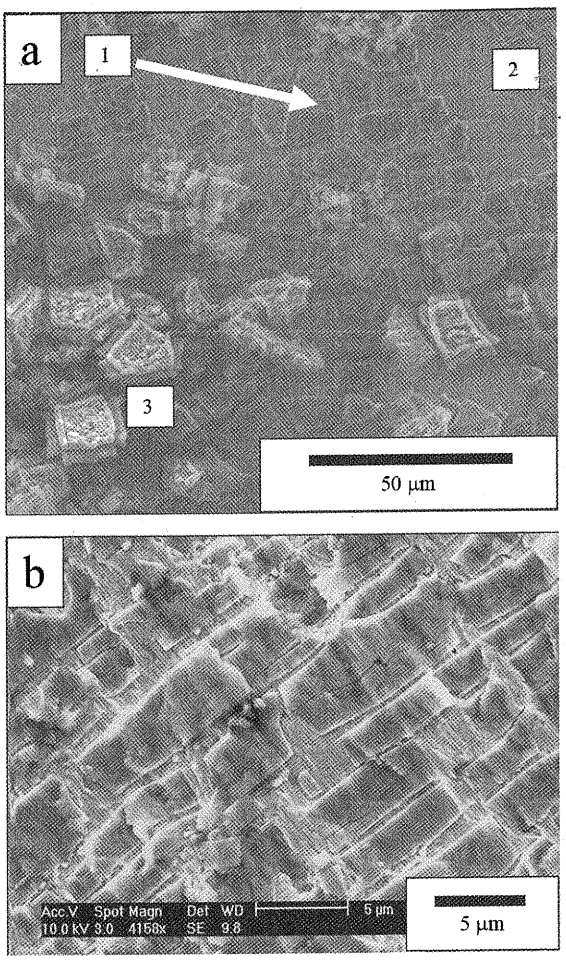

Figure 2. SEM morphology of (a) 1-μm Si film after 30th charge at ~C/2.5 rate, and (b) 250-nm Si film after undergoing severe tensile test conditions.

islands (~10 μm diam) which appear to remain well-adhered and have preserved the vital electronic pathway to the Cu substrate. Region 2 is an example of a region in which all of the Si islands have delaminated from the substrate, isolating the electronic pathways of Si contact to the underlying Cu, thus no longer participating in the redox reactions. Finally, region 3 illustrates piling and accumulation of the debonded Si platelets, the cause of which is unclear at present. Some reasons could be postulated. It is possible that the

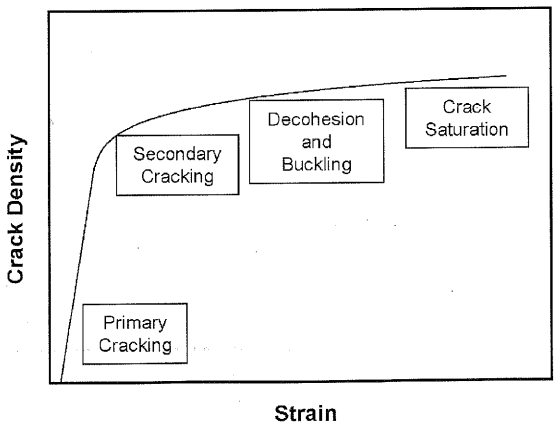

Figure 3. Potential damage regimes that may occur upon uniaxially straining the film/substrate system.

Table I. Strain values at the onset of cracking and onset of debonding in 250-nm a-Si/Cu.

	Before Expt.	Cracking onset	Debond onset
Longitudinal strain (%)	0%	0.5 ± 0.2	2.33 ± 0.4
Transverse strain (%)	0%	−0.5 ± 0.3	−1.5 ± 0.2

delaminated Si plates migrate during cycling which then pile up due to release of the interfacial energy. Another possibility is that accumulation could occur during the disassembly process. Beaulieu et al.[8] have reported observing similar island formation and delamination events in Sn films. Because the failure mode is by delamination rather than crumbling or pulverization of the active material, the as-deposited adhesion strength between Si and Cu was experimentally determined to decipher if the bond strength was high or low.

Interface fracture energy measurement.— There are many experimental methods available to measure the interface fracture energy between a film and substrate, such as the superlayer test method[16] which was developed for metal thin films on nonmetallic substrates. However, few methods are suitable for determining the interface fracture energy of elastic films deposited on elastic–plastic substrates. A method described by Ignat[15] for determining the adhesion strength between brittle chemical vapor deposited films and metallic substrates was adopted to determine the as-deposited adhesion strength between Si and Cu. The method consists of straining the film/substrate system in uniaxial tension while observing the morphology and damage progress of the films in situ in a scanning electron microscope. The possible damage regimes are shown in Fig. 3 and discussed below. In particular, to determine the interface fracture energy, one must know the strain at which the first buckling-induced debond occurs. One must also accurately measure the lateral dimensions of the debond zone. In order to measure the strain required for debond, a suitable area of the film was selected for observation and observed throughout the tensile test. The longitudinal and transverse directions are defined as parallel and normal to the tensile axis, respectively. By measuring the changes in length between surface asperities on the film in both the longitudinal and transverse directions, strains were calculated. For each direction on each micrograph, five measurements were made. The average strain and standard deviation for the onset of both cracking and debonding are reported in Table I. An example of a rectangular debond area is shown in Fig. 4 for a 250-nm Si thin film with the cracks running

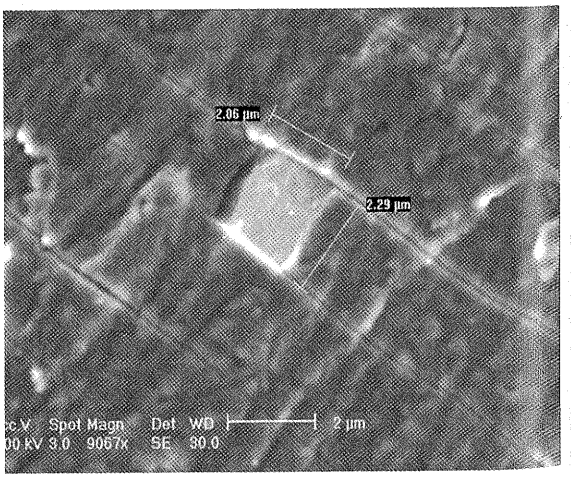

Figure 4. SEM micrograph of 250-nm a-Si thin film on Cu foil showing the area of the debond zone and cracks normal to the tensile axis.

Table II. Intrinsic, experimental, and calculated parameters used to calculate the interfacial fracture energy in 250-nm sputtered a-Si on Cu foil.

Parameter	Value
h	250 nm
ε_{cy}	$-1.5 \pm 0.2\%$
a, b	2.06 μm, 2.29 μm
k	4.04
ν_f	0.22[19]
ε_{calc}	4.2%
ε^*_{cy}	$-2.7\% \pm 0.2\%$
E_f	80 ± 20 GPa[19]
γ	7.7 ± 1.9 J m^{-2}

perpendicular to the tensile axis. The interfacial fracture energy is calculated using an energetic approach developed by Chow et al.[17] to measure the adhesion strength of amorphous selenium vacuum deposited onto polymeric substrates. The analytical formula for the interfacial fracture energy was derived by Chow et al.[17] to be

$$U = \frac{h}{2}\frac{E_f}{1-\nu_f^2}\varepsilon_{cx}^{*2} \quad [1]$$

where ε^*_{cx} is the critical longitudinal strain applied to the system to induce debonding, h is the thickness of the film, and E_f and ν_f are the modulus and Poisson's ratio of the film, respectively. In the present case, debonding of the film occurs by the buckling of the strips of cracked Si film under the effect of the transverse contraction of the Cu substrate. Although the films are in a state of compressive stress upon deposition, the stresses developed during the tensile experiment quickly relieve the as-deposited stress. With residual stress effects being neglected, the critical transverse strain to induce debonding, ε^*_{cy}, is determined from the difference between the experimentally determined transverse strain, ε_{cy}, and the critical buckling strain deduced theoretically, ε_{calc}. Therefore

$$\varepsilon^*_{cy} = \varepsilon_{cy} - \varepsilon_{calc} \quad [2]$$

ε_{calc} was derived for a flat rectangular plate by Timoshenko and Gere[18] to be

$$\varepsilon_{calc} = \frac{k\pi^2}{12(1-\nu_f^2)}\frac{h^2}{b^2} \quad [3]$$

where a is the width of the debond region, b is the length of the debond region (edge of the buckle), and k is a function of the ratio a:b. Although the value obtained for ε_{calc} using Eq. 3 is positive, one must consider ε_{calc} to be negative due to the nature of the strain-induced buckling process. Considering the appropriate value of k from the various a:b ratios given in the text by Timoshenko and Gere,[18] the interfacial fracture energy relation can be rewritten as

$$\gamma = \frac{h}{2}\frac{E_f}{(1-\nu_f^2)}(\varepsilon_{cy} - \varepsilon_{calc})^2 \quad [4]$$

A summary of the relevant intrinsic, experimental, and calculated parameters used to calculate the interfacial fracture energy are shown in Table II. The obtained value for the interfacial fracture energy is 7.7 J ± 1.9 J m^{-2}. This value is very close to the interface fracture toughness of 8 J m^{-2} obtained by Volinsky[20] for Al–Cu films on a Si substrate tested with a W superlayer. Assuming that the thermodynamic work of adhesion between Si and Cu is in the same range (0.1–3 J m^{-2}) as those of the solid-state metal/ceramic interfaces studied by Hondros,[21] the work of adhesion is only a portion of the total interface fracture toughness. The other contribution must come from irreversible energy dissipation processes. For example, the plastic flow in the Cu at the interfacial crack tip is certainly a plausible contributor to the measured energy value. Furthermore, the measured energy value is also a strong function of the trajectory of the interfacial crack, which is dependent on the test method.[22] Further consideration of the phase angle, ψ, for the present tensile testing method will require further analysis, the results of which will be published at a future date.

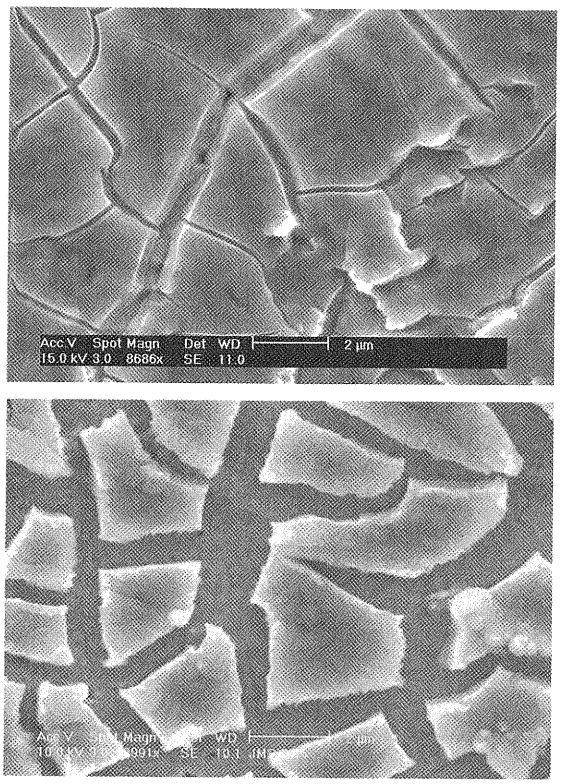

Figure 5. Plan-view SEM micrograph of 250-nm Si film cycled at ~C/2.5 for (a) 1 cycle and (b) 30 cycles.

After noting that energy dissipation from plastic flow in the substrate could most likely contribute to a substantial fraction of the adhesion strength between the a-Si and Cu substrate, 250-nm samples were cycled for 1 cycle and 30 cycles to determine if the expansion/contraction of the active material could cause plastic deformation of the substrate. Figure 5a and b show the plan-view SEM images of the 250-nm Si films deposited on Cu substrate after electrochemical cycling at ~C/2.5 for 1 cycle and 30 cycles, respectively. From Fig. 5a, it can be easily distinguished that the film has undergone fracture and cracks have emerged after the first cycle itself. As shown in Fig. 6a and b, in situ AFM performed on a 250-nm Si film during the first lithiation half-cycle clearly shows that the film expands laterally during the first lithiation. Figure 6a and b was acquired before the first major lithiation reaction and after most of the lithiation reactions were completed, 290 and 119 mV, respectively. Depending on the direction measured (each line represents a measurement between two surface features or asperities on the film), the expansion varied between 0.8 and 3.7%. Using a simplified approach which approximates the stress as $\sigma = E\varepsilon$, and using a value of E = 80 GPa[19] for an amorphous silicon thin film, we obtain a range of stress 640 MPa $< \sigma <$ 3.0 GPa. A more refined estimate of the stress generated during lithiation may aid in future substrate materials selection/design. The shear modulus of copper at room temperature is 74 GPa, and its ideal shear strength may be estimated at 5% of the shear modulus.[23] Therefore, the ideal shear strength of copper is about 3.7 GPa at room temperature. Our lithiation-induced stress is ~3.0 GPa. Plastic deformation is probable because the stress developed during the first lithiation is on the order of shear strength of copper. The AFM and SEM analyses indicate that during the first lithiation half-cycle, the Si expands both in thickness and in the plane of the film. During the process of active

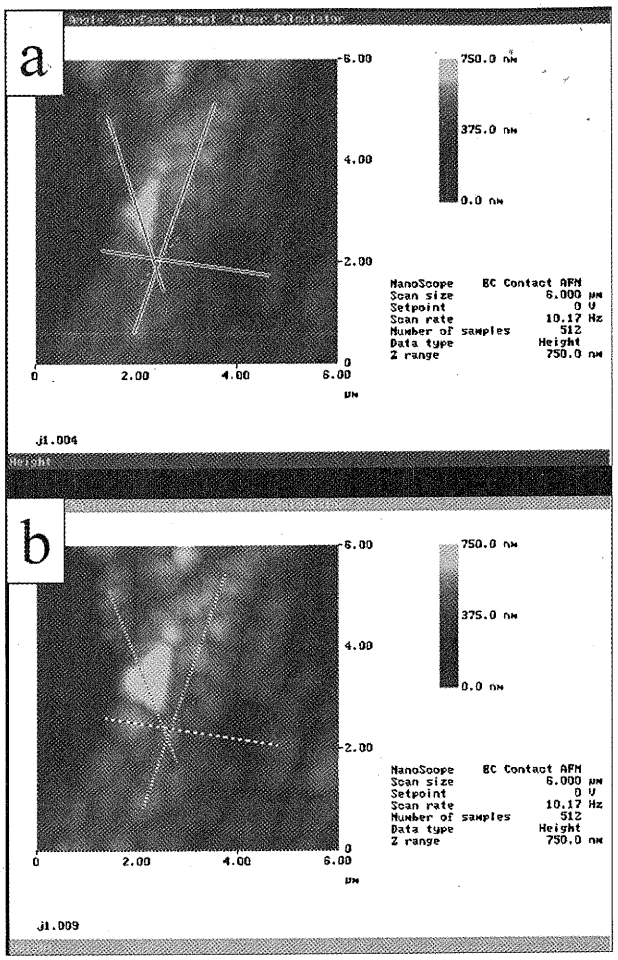

Figure 6. In situ AFM images of a 250-nm Si film on Cu foil taken during the first lithiation half-cycle at (a) 290 and (b) 119 mV.

material expansion, the compressive stress of the film would increase in magnitude due to the constraint placed on the film by the attached substrate. At some point during the first cycle, the compressive stress in the film is large enough to induce buckling and cause compressive failures or cracks in the film similar to those described by Thouless.[24] One must also remember that a-Si has been proven by Beaulieu et al.[25] to exhibit conservation of volume during a lithiation/delithiation cycle. Therefore, assuming that the substrate area occupied by the silicon before and after the 1st cycle remains the same, one can argue that the area of the Cu substrate has increased and that an irreversible plastic strain has been experienced by the Cu, leading to the gaps between Si seen in Fig. 5a. If subsequent cycling leads to elastic strain in the substrate, then one would expect to see no increase in the gap between Si "islands". However, if the gaps are observed to widen as in the present case, it is reasonable to mention that there exists an incremental plastic strain in the Cu with the increase in cycle number. From the post-30-cycle Si film sample shown in Fig. 5b, it can be construed that the gaps between the Si islands indeed widen substantially by the 30th cycle. Keeping in mind the Si volume is conserved upon cycling, the negligible reversible capacity loss between the 1st and 30th cycle, and the widening gaps between Si islands, it appears that there is electrochemical volume expansion/contraction-induced incremental plastic strain in the Cu substrate. Such incremental plastic strain has not been previously reported in lithium-ion battery anode systems. However, the concept of incremental plastic strain upon cycling, commonly called ratcheting, is well-known in other fields such as thermal barrier coatings[13] and Si chip packaging technology.[14] The phenomenon seen in our case for the active Si and inactive Cu is

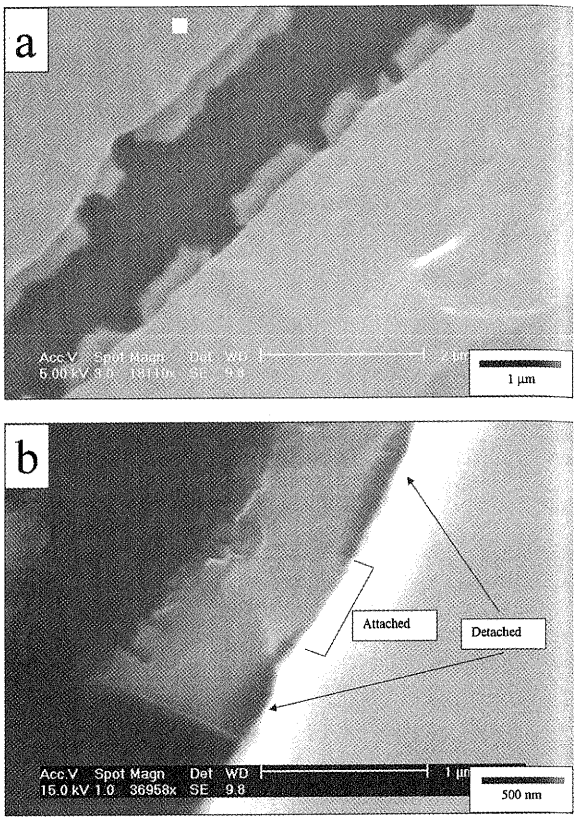

Figure 7. Cross-sectional SEM micrograph of 250-nm Si film cycled at ~C/2.5 for (a) 3 cycles and (b) 30 cycles.

also similar to the ratcheting observed in fiber-reinforced aluminum matrix composites which experience thermal cycling and transverse stresses.[26]

Although ratcheting in the Cu explains the widening gaps between the Si islands, it does not explain the eventual delamination of the compressively stressed Si islands. For delamination to occur in a compressively stressed film on a substrate, an initial decohesion from an interface imperfection needs to be present.[27] In order to determine if the failure mode of the films is indeed preceded by the presence of an imperfection, the morphology of the interface was analyzed by SEM. Figure 7a and b shows the cross-sectional SEM results for 250-nm Si film samples observed after 3 and 30 cycles, respectively. Figure 7a shows that after three cycles, the islands of Si are still well attached to the Cu substrate and no evidence of interface imperfections is seen. Figure 7b is more revealing because it is very close to the event at which the 250-nm Si films usually begin to fail. One can see that the Si island is detached in two areas but still remains adhered in one region that is approximately 300 nm in length. Researchers have mentioned although never demonstrated evidence of such adhesion retention in Sn thin films by a small area near the active material island's center.[8] A more detailed analysis in the form of cross-sectional scanning TEM (STEM) was undertaken on an as-deposited and a Si film after subjecting it to 30 cycles to investigate possible formation of an interface imperfection that could result in the final failure of the Si islands. The cross-sectional images of the as-deposited and the film after 30 cycles are shown in Fig. 8a and b, respectively. Distinct contrast variations are observed near the interface in the cycled sample that are not present in the as-deposited sample. This suggests that there could possibly be the formation of an interfacial phase between the Cu and Si during electrochemical cycling. Energy-dispersive X-ray (EDX) line profiles for Cu and Si were collected along the line crossing the film-substrate interface shown in Fig. 8a and b. The results of the EDX line profiles are shown in Fig. 8c and d for the as-deposited and

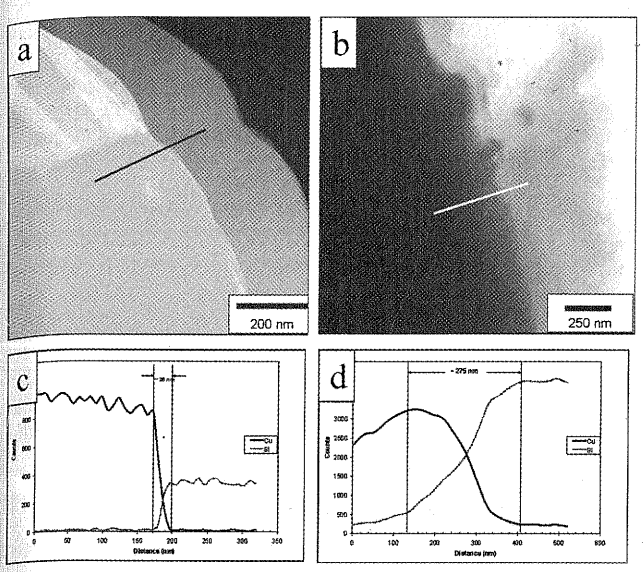

Figure 8. Cross-sectional STEM images of 250-nm Si film (a) as-deposited and (b) cycled at ~C/2.5 for 30 cycles, and the corresponding Cu and Si EDX line profiles for the (c) as-deposited Si film and (d) Si film cycled at ~C/2.5 for 30 cycles (position lines shown in (a) and (b), respectively).

cycled samples, respectively. The EDX line profiles clearly indicate that atomic intermixing has occurred between the film and substrate, with the interfacial region expanding from ~26 nm in the as-deposited film to ~275 nm in the sample subjected to 30 cycles. The formation of the most likely copper–silicon phase (Cu_3Si) was not observed, as noted from the absence of plateaus in the EDX line profiles of Cu and Si in the interfacial region. To corroborate this evidence of an interface phase, the 250-nm Si thin film was galvanostatically cycled at a very slow rate of ~C/12.5 to observe any potential phase formation, which is indicated by a sharp peak in the calculated differential capacity plot. Figure 9a shows the specific capacity vs cycle number for the 250-nm Si film cycled at C/12.5, and the corresponding differential capacity plots for cycles up to the 22nd, 25th, and 30th cycles are displayed in Fig. 9b-d, respectively. The 250-nm Si film appears to fail earlier at a very slow cycle rate with the failure starting around the 23rd cycle, as noted by a decrease in the Coulombic efficiency for that cycle. By observing the discharge portion of the *dQ/dV* graphs, one can notice an increasing anomalous sharp peak occurring during delithiation in the 25th and 30th cycles at around 0.42 V, which normally is indicative of a Li–Si phase. However, such a peak has never been observed by us or reported by others in normal bulk Si anodes. Correlating the above STEM results with the *dQ/dV* results, the presence of this peak could therefore suggest the nucleation of a lithium copper silicide crystalline phase that must weaken the remaining interfacial region between Si and Cu, leading to failure due to loss of electrical contact between the active material and current collector. Preliminary analysis in the form of plan-view selected area electron diffraction (SAED) on postcycled Si/Cu samples is shown in Fig. 10a and b. Figure 10a shows the plan-view bright field TEM image of a 250-nm Si thin-film island region after 30 cycles at C/2.5 (just before failure). Figure 10b illustrates the SAED pattern of the outlined

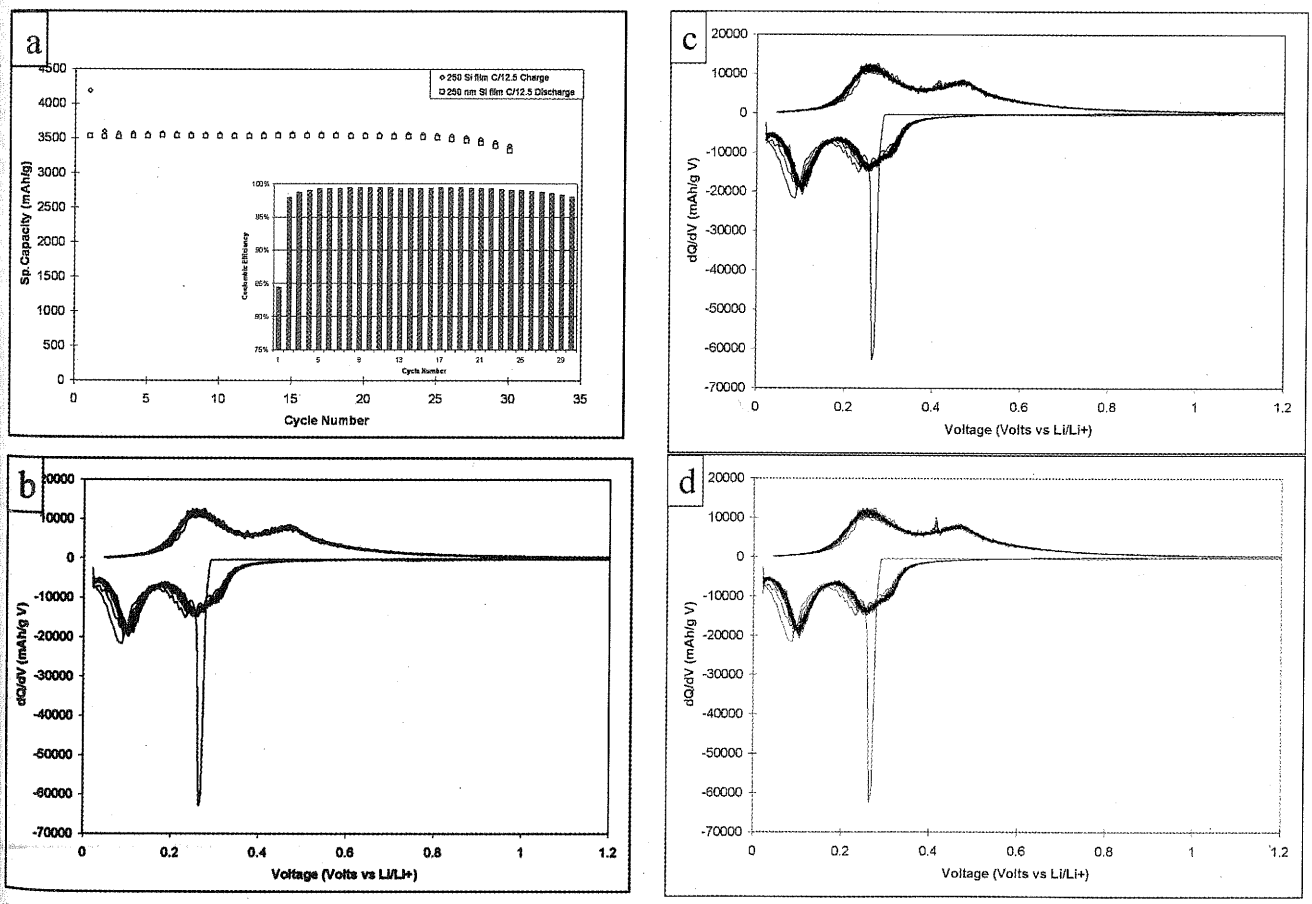

Figure 9. Electrochemical cycling results of 250-nm Si thin film cycled at ~C/12.5 rate for 30 cyles: (a) specific capacity vs cycle number (overlay - Coulombic efficiency vs cycle number), (b) differential capacity plot for the 1st - 22nd cycles, (c) differential capacity plot for the 1st - 25th cycles, and (d) differential capacity plot for the 1st - 30th cycles.

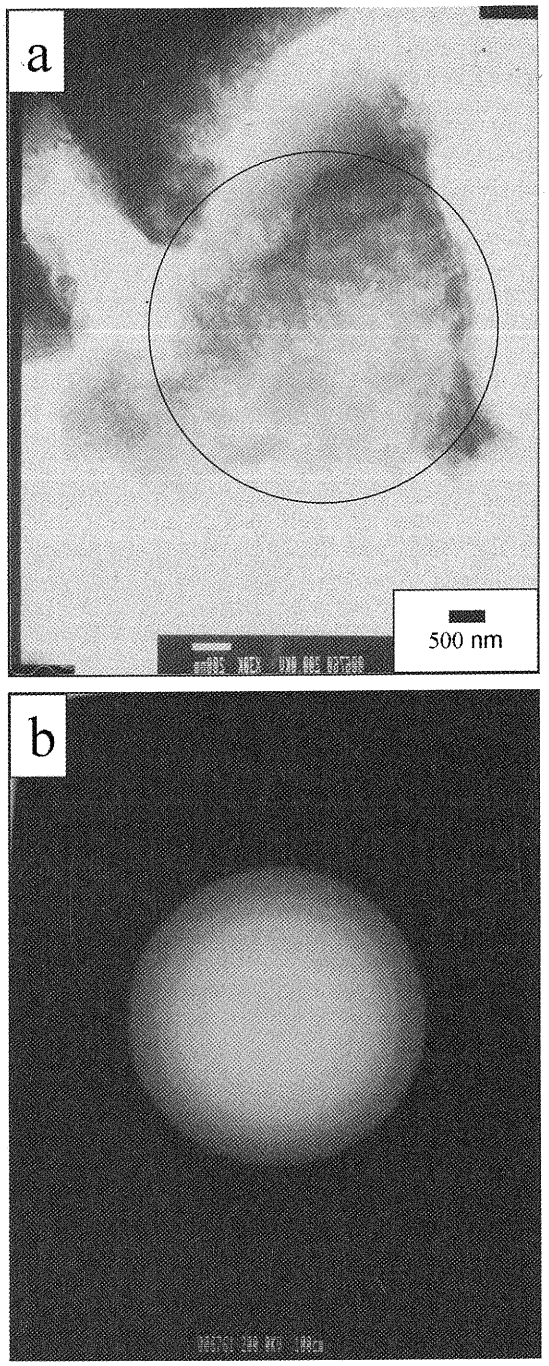

Figure 10. TEM analysis of 250-nm Si thin film after 30 cycles at C/2.5 (a) plan-view bright field image, and (b) SAED pattern with $L = 100$ cm of circular region shown in (a).

region of Fig. 10a. The two denoted rings in the SAED pattern match very closely with the two strongest diffracting planes of Cu_2LiSi, JCPDS[28] pattern no. 71-2329; however, a more detailed study is warranted to make final confirmation of the suspect imperfection phase. Furthermore, more studies on the morphology and microstructure of the lithium-inserted Si film would be valuable to comprehensively understand the interface phenomenon.

Following the observation of ratcheting in the Cu substrate material and potential failure due to interfacial phase formation, several design recommendations can be suggested to improve the properties of the active-inactive thin-film anode systems. In order to combat the effects of ratcheting, such as interfacial crack extension and void formation in the substrate, techniques may be adopted that have been useful in the field of metal matrix composites with interface layers. Jansson and Leckie[29] calculated that an interfacial layer between a fiber and matrix should have a very low modulus to improve the cyclic temperature properties of the composite. In our case, an interfacial layer with a very low modulus could be used to mitigate the volumetric change-induced stresses in the anode system. The use of compliant matrix materials has been put forth in the case of bulk powder lithium-ion anode systems.[7] The use of materials in thin-film multilayers that may act in a compliant matrix manner has also been examined in several research studies that indicate promising feasibility in such systems.[10,30,31] Finally, the interfacial layer should be an effective diffusion barrier layer to prevent the formation of amorphous Cu–Si phases that can lead to potential formation of detrimental crystalline phases during the delithiation process. These are potential design and materials considerations, the implementation and analysis of which will be part of subsequent publications.

Conclusion

Amorphous silicon thin films on copper foil have been observed to exhibit high, near theoretical capacities for a limited number of cycles. The adhesion strength of the a-Si on polycrystalline Cu foil interface fracture energy has been measured to be 7.7 J m^{-2}, which is greater than the expected value of the thermodynamic work of adhesion, indicating contributions from Cu substrate plasticity. For the first time in an electrochemical active/inactive anode system, ratcheting has been reported in which the inactive metal material undergoes an incremental increase in plastic strain with cycle number. The islands of Si formed during the first cycle remain in a state of compressive stress during subsequent cycling, leading to the requirement that an interface imperfection must be present to cause final decohesion of the Si island. Combined with STEM and EDX line profiles indicating interdiffusion of Cu and Si during electrochemical cycling, the appearance of a sharp peak at ~0.42 V (delithiation half-cycle) during slow-scan-rate cycling of a 250-nm Si film in the cycle at which failure (delamination) initiates suggests that the most likely interface imperfection leading to failure is a lithium copper silicon phase. A diffusion barrier interface layer that has a very low modulus may improve the cycle life of the a-Si thin film on polycrystalline Cu substrate anode system and any other analogous battery systems.

Acknowledgments

J.P.M. and P.N.K. acknowledge the support of NASA (GSRP and NAG3-2640), Chang's Ascending (Taiwan), NSF (CTS-0000563), and ONR (grant N00014-00-1-0516).

Carnegie Mellon University assisted in meeting the publication costs of this article.

References

1. M. Winter and J. O. Besenhard, *Electrochim. Acta*, **45**, 31 (1999).
2. Y. Idota, T. Kubota, A. Matsufuji, Y. Maekawa, and T. Miyasaka, *Science*, **276**, 1395 (1997).
3. R. A. Huggins, *J. Power Sources*, **81-82**, 13 (1999).
4. J. Yang, M. Winter, and J. O. Besenhard, *Solid State Ionics*, **90**, 281 (1996).
5. R. A. Huggins, *Solid State Ionics*, **113-115**, 57 (1998).
6. W. J. Weydanz, M. Wohlfahrt-Mehrens, and R. A. Huggins, *J. Power Sources*, **81-82**, 237 (1999).
7. O. Mao, R. L. Turner, I. A. Courtney, B. D. Fredericksen, M. I. Buckett, L. J. Krause, and J. R. Dahn, *Electrochem. Solid-State Lett.*, **2**(1), 3 (1999).
8. L. Y. Beaulieu, K. W. Eberman, R. L. Turner, L. J. Krause, and J. R. Dahn, *Electrochem. Solid-State Lett.*, **4**, A137 (2001).
9. L. Y. Beaulieu, K. C. Hewitt, R. L. Turner, A. Bonakdarpour, A. A. Abdo, L. Christensen, K. W. Eberman, L. J. Krause, and J. R. Dahn, *J. Electrochem. Soc.*, **150**, A149 (2003).
10. J. Kim, H. Lee, K. Lee, S. Lim, and S. Lee, *Electrochem. Commun.*, **5**, 544 (2003).
11. J. Maranchi, A. Hepp, and P. Kumta, *Electrochem. Solid-State Lett.*, **6**, A198 (2003).
12. S. Jansson and F. Leckie, *J. Mech. Phys. Solids*, **40**, 593 (1992).
13. M. Huang, Z. Suo, Q. Ma, and H. Fujimoto, *J. Mater. Res.*, **15**, 1239 (2000).
14. M. He, A. Evans, and J. Hutchinson, *Acta Mater.*, **48**, 2593 (2000).
15. M. Ignat, *Chemical Vapor Deposition*, ASM International, Surface Engineering Series, Vol. 2, J. Park, Editor, pp. 45-80, ASM International, Metals Park, OH

(2001).
16. A. Bagchi, G. E. Lucas, Z. Suo, and A. G. Evans, *J. Mater. Res.*, **9**, 1734 (1994).
17. T. Chow, C. Liu, and R. Penwell, *J. Polym. Sci., Part A-1*, **14**, 1305 (1976).
18. S. Timoshenko and J. Gere, *Theory of Elastic Stability*, p. 355, McGraw Hill, New York (1961).
19. L. B. Freund and S. Suresh, *Thin Film Materials*, p. 96, Cambridge University Press, New York (2003).
20. A. Volinsky, Ph.D. Thesis, University of Minnesota, Minneapolis, MN (2000).
21. E. Hondros, *Inst. Phys. Conf. Ser.*, **75**, 121 (1986).
22. A. G. Evans, B. J. Dalsleish, M. He, and J. W. Hutchinson, *Acta Metall.*, **37**, 3249 (1989).
23. D. Agrawal and R. Raj, *Acta Metall.*, **37**, 1265 (1989).
24. M. D. Thouless, *J. Am. Ceram. Soc.*, **76**, 2936 (1993).
25. L. Y. Beaulieu, T. D. Hatchard, A. Bonakdarpour, M. D. Fleischauer, and J. R. Dahn, *J. Electrochem. Soc.*, **150**, A1457 (2003).
26. S. Jansson and F. Leckie, *J. Mech. Phys. Solids*, **40**, 593 (1992).
27. M. Y. He, A. G. Evans, and J. W. Hutchinson, *Mater. Sci. Eng., A*, **245**, 168 (1998).
28. Card no. 71-2329, JCPDS-International Center for Diffraction Data, Swarthmore, PA (2001).
29. S. Jansson and F. Leckie, *J. Compos. Mater.*, **26**, 1474 (1992).
30. Y. Kim, H. Lee, S. Jang, S. Lim, S. Lee, H. Baik, Y. Yoon, and S. Lee, *Electrochim. Acta*, **48**, 2593 (2003).
31. S. Lee, H. Lee, Y. Park, H. Baik, and S. Lee, *J. Power Sources*, **119-121**, 117 (2003).